Slow coarsening of $B2$-ordered domains at low temperatures: A kinetic Monte Carlo study

D. Le Floc'h* and P. Bellon†
Department of Materials Science and Engineering, Frederick Seitz Materials Research Laboratory, Urbana, Illinois 61801

M. Athènes
DECM/SRMP, CEA-Saclay, Gif-sur-Yvette 91191, France
(Received 12 July 1999; revised manuscript received 16 March 2000)

The kinetics of the ordering and coarsening of $B2$-ordered domains is studied using atomistic kinetic Monte Carlo simulations. Special emphasis is put on the effect of annealing temperature, alloy composition, and atom dynamics on the coarsening behavior. When atomic diffusion proceeds by vacancy jumps to nearest-neighbor sites, a transient slow coarsening regime is observed at temperatures below half the order-disorder transition temperature T_c. It results in apparent coarsening exponents that decrease with decreasing the annealing temperature. Values as low as 0.14 are measured at $0.25T_c$. Slow transients take place in both stoichiometric and nonstoichiometric alloys. These regimes are correlated with the transient creation of excess antisites during domain disappearance. Since antiphase boundary mobility decreases with increasing antisite concentration, this transient excess results in the slow coarsening observed in simulations.

I. INTRODUCTION

The kinetics of domain growth and coarsening has been a subject of great attention in materials science. Indeed, these phenomena play an important role in alloys since the size and morphology of domains are essential parameters in determining the properties of the use of materials. In this paper we concentrate on the ordering and coarsening of ordered domains when a high-temperature disordered phase is cooled through a continuous (here second-order) ordering transition line and isothermally annealed. We investigate in particular the effect of annealing temperature.

During such an ordering reaction, the long-range order parameter describing the transformation is not conserved, and the classical theory developed by Allen and Cahn[1] predicts that the velocity of antiphase boundaries (APBs) is proportional to their curvature and that in the late stages ordered domains coarsen following a power law $L \propto t^{1/2}$, where L is the average domain size and t the annealing time. This asymptotic coarsening regime should be obtained regardless of the annealing temperature.

At low temperatures, however, phenomena not considered in the Allen-Cahn theory may take place and thus modify the coarsening behavior. One example is the faceting of APBs below their roughening transition temperatures. Indeed, at a facet the local APB mean curvature is zero and its velocity according to the Allen-Cahn description should go to zero. In fact, such a faceted APB will move by the nucleation and growth of kinks. Castan and Lindgard[2] have shown that in the presence of a mixture of curved and flat interfaces, coarsening at very low temperatures may be described by a new universality class with a coarsening exponent of 1/4. On the other hand, Lai, Mazenko, and Valls[3] have proposed a classification of coarsening regimes based upon the nature of activation barriers that exist for coarsening. If the activation energy to nucleate and propagate a kink at the edge of a facet is independent of the length of the edge (class-2 model), a classical Allen-Cahn behavior is expected asymptotically. However, when this activation energy grows with the edge length (class-3 and -4 models), logarithmic laws are expected. Shore *et al.*[4] have obtained simulation results on model systems that strongly support such predictions.

Long-lived transients may also appear at low annealing temperatures. Specific transient domain morphologies, e.g., the formation of minimal surfaces[5] or necking,[6] are expected to slow down coarsening rates. Furthermore, for a class-2 system, a slower coarsening rate is expected to take place for times shorter than the characteristic time to overcome diffusional barriers.

In the case of nonstoichiometric alloys, the coarsening behavior can also be affected by majority species segregation at APBs. In the model proposed by Krzanowski and Allen[7] where coupling between the concentration and degree of order fields is neglected, the presence of segregation, in the low-APB-velocity limit, is shown to reduce the mobility of APBs, however without affecting the coarsening exponent. More recent mean-field computer simulations[8] where the coupling between composition and degree of order fields is taken into account indicate that the APB mobility is indeed reduced by segregation, but also becomes time dependent, reflecting the local chemistry evolution at an APB during its motion. This time-dependent mobility may result in an apparent coarsening exponent different from 1/2, although no specific calculations have been performed in that direction by Dobretsov *et al.*[8] For the sake of completeness, let us mention that in the case where the APBs are fully wetted by majority species, APB motion becomes limited by the transport of this wetting layer, and the coarsening is then predicted to follow a power law with a 1/3 exponent, in good agreement with experiments on Fe-Al alloys.[9]

Many ordered alloys, including Ni_3Mn, Cu_3Au, Ni_3Fe, FeAl, Fe_3Al, and Ni_4Mo, have been studied to test the validity of the Allen-Cahn coarsening regime. The main results in terms of the coarsening exponent have been recently summarized by Frontera *et al.*[10] (see their Table 3). Apparently, most of the results are consistent with the Allen-Cahn theory. For instance, in the case of Cu_3Au (Ref. 11) (which exhibits a first-order transition) annealed at temperatures ranging

 ©2000 The American Physical Society

from $0.97T_c$ to $0.99T_c$ and in the case of Fe_3Al (Ref. 12) (which exhibits a second-order transition) annealed at temperatures ranging from $0.92T_c$ to $0.99T_c$, coarsening exponents very close to 1/2 have been obtained (T_c is the order-disorder transition temperature of the alloy investigated). We want, however, to stress that almost all experiments have been performed above $0.9T_c$. This is because below T_c chemical ordering suppresses atomic diffusion, leading to slow coarsening rates. Some studies performed at low temperatures tend to indicate that the apparent coarsening exponent decreases with decreasing temperature. For instance, an exponent close to 1/2 has been measured in Ni_4Mo at temperatures above $0.94T_c$, but the value dropped to 0.35 at $0.85T_c$ and $0.76T_c$.[13] A similar decrease has been reported in early studies on Cu_3Au.[14] In addition to the faceting and segregation phenomena discussed above, impurity segregation and stress effects could also contribute to such a slowing down.

In the last two decades, atomistic computer simulations have been used intensively to study ordering reactions and, in particular, to test the Allen-Cahn coarsening regime. For a simple cubic lattice of 30^3 sites, with first-nearest-neighbor atomic interactions, Phani *et al.*[15] reported a coarsening exponent compatible with 1/2 during an annealing at $0.59T_c$ using an atom-exchange dynamics. Vives and co-workers, using a dynamics that includes both nearest-neighbor and next-nearest-neighbor vacancy-atom exchanges and with a Metropolis algorithm, observed a strong effect of the annealing temperature on the coarsening exponents for the square lattice[16] and for the body-centered-cubic (bcc) lattice.[10] In both cases, the coarsening exponent is found to be close to 1/2 near T_c, but to increase towards unity as the annealing temperature is decreased. According to the authors, this strong effect is not observed on the square lattice when the atom dynamics proceeds by direct atom exchange, for which the classical 1/2 exponent is found. The authors also claim that if only nearest-neighbor vacancy exchanges are permitted, a logarithmic coarsening is observed for the square lattice. More recently, Frontera *et al.*[17] have reported on the coarsening of $L1_2$ ordered phases on a face-centered-cubic (fcc) lattice, using either a direct atom-exchange dynamics or a nearest-neighbor vacancy-atom-exchange dynamics, in both cases with a Metropolis algorithm. For both dynamics coarsening exponents close to 1/2 are obtained at $0.83T_c$, but lower values are measured at $0.55T_c$, ranging from 0.26 to 0.41. No explanation has been proposed to account for such low values. The same authors also show that isotropic scaling of the structure factor holds for the vacancy dynamics, whereas anisotropic scaling is required for the atom-exchange mechanism. Using a three-state Blume-Emery-Griffiths (BEG) model on a two-dimensional (2D) square lattice, Porta *et al.*[18] have shown that vacancy-vacancy interactions lead to algebraic growth with exponents smaller than 1/2, whereas asymmetry in the atom-atom interactions do not produce a deviation from the Cahn-Allen value in the asymptotic regime.[19] These last two results have been obtained when vacancies are allowed to exchange with nearest and next-nearest neighbors. When only nearest-neighbor exchanges are allowed, no quantitative analysis is available, but very different evolutions are observed due to the trapping of vacancies inside ordered domains.[10]

These differences in simulation results clearly indicate the strong role played by the atom dynamics chosen. In most ordered phases atomic diffusion proceeds by vacancy jumps, each jump being thermally activated. From a metallurgical point of view, it is therefore clear that one should use algorithms that generate system evolution via thermally activated migration of vacancies. Recently, residence time algorithms have been introduced for that purpose.[20] In these algorithms evolutions of microstructures are, by construction, obtained as a function of a physical time unit, as opposed to Monte Carlo step units used in the standard Metropolis algorithm. Furthermore, at low temperatures these algorithms are exempt from the high rejection rates observed in conventional Metropolis simulations. Higher-order residence time algorithms have also been introduced to circumvent the problem of vacancy trapping in ordered domains.[21] Kinetic Monte Carlo simulations based on a first-order residence time algorithm have been used in this work to study the effect of annealing temperature on the coarsening kinetics of a $B2$-ordered phase. Preliminary results[22,23] indicated that at temperatures roughly below $0.5T_c$ coarsening is strongly slowed down. This effect is studied in detail here, as well as the influence of the alloy composition and the atom dynamics on this slowing down.

The paper is organized as follows: In Sec. II, the model alloy and the simulation technique are briefly recalled. In Sec. III, microstructural evolutions during isothermal annealing are presented and analyzed. These results are then discussed in Sec. IV.

II. ATOMISTIC KINETIC MODEL

We recall briefly here the atomistic kinetic model that has been already presented in detail elsewhere.[24] A rigid bcc lattice is considered, with periodic boundary conditions; for computer efficiency, atomic positions are given in a rhombohedral frame with one atom per unit cell and N^3 lattice sites. The binary alloy consists of N_A A atoms, N_B B atoms, and one vacancy (unless stated otherwise) distributed over 256^3 lattice sites. Atomic interactions are modeled by pair energies ε_{XY} between nearest-neighbor sites, where X,Y equals A or B. These interactions are here limited to first nearest neighbors. This alloy exhibits a second-order $A2$-$B2$ order-disorder transition with a critical temperature $T_c = 0.794 \times 2\varepsilon$ (Ref. 25) at the $A_{50}B_{50}$ stoichiometric composition, where the ordering energy ε is defined as $\varepsilon = \varepsilon_{AA} + \varepsilon_{BB} - 2\varepsilon_{AB}$.

Atomic diffusion proceeds by nearest-neighbor exchange with the vacancy, and the rate of these exchanges is calculated using rate theory. A constant preexponential term is chosen for simplicity, and the activation energy for an atom-X–vacancy exchange, $\Delta E_{XV}^{\mathrm{act}}$, is calculated using a broken-bond model:

$$\Delta E_{XV}^{\mathrm{act}} = E_s - \sum_{Y \in nn(X)} \varepsilon_{XY}, \tag{1}$$

where E_s, the contribution of atom X to the energy of the crystal at the saddle point position, is taken as a constant. The sum in Eq. (1) runs over all the atoms that are a nearest neighbor of X. For the sake of simplicity, we will here re-

strict ourselves to the case where $\varepsilon_{AA}=\varepsilon_{BB}$; our previous results[23] indicate that moderate asymmetries in atomic interaction, i.e., $|\varepsilon_{AA}-\varepsilon_{BB}|<\varepsilon$, do not change qualitatively the main trend of the results described in this paper. This is consistent with recent results reported by Porta *et al.*[19] for a BEG model. The time evolution of the alloy is built using a first-order residence time algorithm.[21,24] This algorithm allows for one vacancy jump at each Monte Carlo step. The evolution of the system is followed as a function of the physical time, the scale of which is defined by the vacancy jump frequencies and the vacancy concentration (taken as constant in our simulations). For computational efficiency, the configuration-independent part in the activation energies is factorized out. Simulation times are thus given in an arbitrary time scale, and for comparison with experiments one would have to correct it by this factorized term and by the actual vacancy concentration. This model, with some minor variations, has been successfully used to study the simultaneous precipitation and ordering reactions in binary alloys on fcc (Ref. 20) and bcc (Ref. 24) lattices. It has also been used and directly compared with experiments on the kinetics of the precipitation of Cu in dilute *Fe*-Cu alloys[26] and on the kinetics of the precipitation of the $L1_2$ phase in a ternary Ni-Al-Cr alloy.[27]

The evolution of the system can be followed in direct space by visualizing the positions of the atoms, the degree of order field, or the concentration field. As discussed in Ref. 24, these fields are obtained by counting atoms on a central site and on the first- and second-nearest-neighbor shells around this site. The Warren-Cowley short-range order parameter for first nearest neighbors, α, is also calculated during the simulations.

An alternative way of following the evolution of the system is to compute the structure factor $S(\mathbf{k})$, obtained as the Fourier transform of the pair correlation function of atomic occupancies. Information relative to the order field is obtained by calculating the structure factor $S(\mathbf{k}-\mathbf{k}_s)$ centered around a $B2$ superlattice vector $\mathbf{k}_s$, then taking its spherical average (unless specified otherwise), and calculating its moments. The integrated intensity of the superlattice reflection, I, is obtained by integrating $S(|\mathbf{k}-\mathbf{k}_s|)$ in a volume centered around $\mathbf{k}_s$, such that $|\mathbf{k}-\mathbf{k}_s|<0.1|\mathbf{k}_s|$. The long-range degree of order, S, is given by $S=\sqrt{I/I_{B2}}$, where I_{B2} is the integrated intensity for a perfectly ordered $B2$ phase. The average size of the ordered domains, L, is obtained as $L=\sqrt{M_0/M_2}$, where the moments M_n are defined by

$$M_n=\sum_{k\in\omega}|\mathbf{k}-\mathbf{k}_s|^n S(|\mathbf{k}-\mathbf{k}_s|)/n(|\mathbf{k}-\mathbf{k}_s|), \qquad (2)$$

where ω contains all vectors such that (i) their intensity is above the background level of a random alloy and (ii) $|\mathbf{k}-\mathbf{k}_s|<0.5|\mathbf{k}_s|$; $n(|\mathbf{k}-\mathbf{k}_s|)$ is the multiplicity of that reflection.

III. SIMULATION RESULTS

In the following results, unless stated otherwise, a random configuration is isothermally annealed until very large domain or single-domain structures are obtained. First, in Sec. III A the effect of the annealing temperature on ordering and coarsening is presented for stoichiometric alloys. Then in Sec. III B alloys with off-stoichiometric compositions are studied. Finally, in Sec. III C atom dynamics differing from the vacancy dynamics described in Sec. II is implemented, and the simulation results are contrasted with those obtained in Sec. III A.

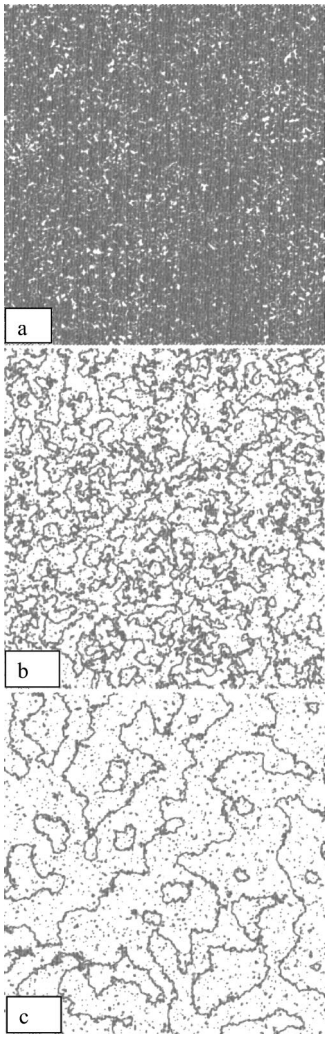

FIG. 1. Absolute value of the local degree of order field in (110) planes. At $T=0.723T_c$, microstructures are shown at times (a) $t=4.3\times10^6$, (b) $t=1.5\times10^8$, and (c) $t=7.2\times10^8$. The vertical dimension of each microstructure corresponds to 256 nearest-neighbor distances. The square of the local order parameter is displayed on a gray scale such that black and white correspond to fully disordered and fully ordered states, respectively.

A. Effect of temperature

1. Microstructural evolutions

Figures 1 and 2 display the evolution of the absolute value of the degree of order field for three annealing times and two temperatures, $T=0.723T_c$ and $T=0.362T_c$, respectively. In both cases, at short times small ordered regions form in the disordered matrix and then grow [Figs. 1(a) and 2(a)], until the disordered matrix has disappeared and thin domain walls have formed almost everywhere [Figs. 1(b) and 2(b)]. This is the end of the ''ordering'' regime, using the terminology of

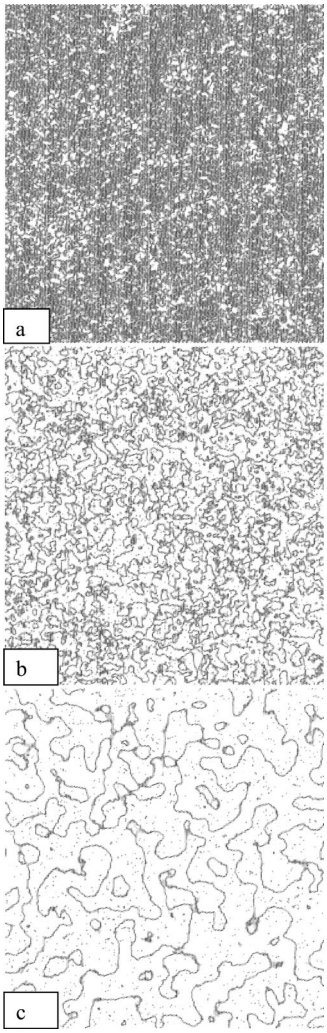

FIG. 2. Absolute value of the local degree of order field in (110) planes. At $T=0.362T_c$, microstructures are shown at times (a) $t=3.3\times10^7$, (b) $t=3.1\times10^8$, and (c) $t=6.9\times10^9$ (arbitrary time units). The vertical dimension of each microstructure corresponds to 256 nearest-neighbor distances. The square of the local order parameter is displayed on a gray scale such that black and white correspond to fully disordered and fully ordered states, respectively.

Nagler *et al.*[11] These microstructures do not correspond to the ones expected by the theory of continuous ordering, which should produce long-wavelength structures.[28,29] Microstructures similar to ours have been reported in simulations of Cu_3Au quenched and annealed at temperatures well below any possible spinodal temperature.[30] Notice that in Figs. 1(b) and 2(b) some coarsening has already taken place, as shown by the presence of a few large domains. This overlap, between ''ordering'' and coarsening regimes, results from the fact that thin boundary walls are not formed everywhere at the same time. At the end of the ''ordering'' regime, the long-range order parameter has reached a value of 0.45 and 0.35, respectively, much smaller than the equilibrium values at these temperatures, 0.90 and 0.99, respectively (the equilibrium values are measured on single-domain structures at the end of the simulations). These low degrees of order come not only from the high volume fraction of APBs, but also from the presence of many antisites in excess inside the domains. This point will be discussed in detail

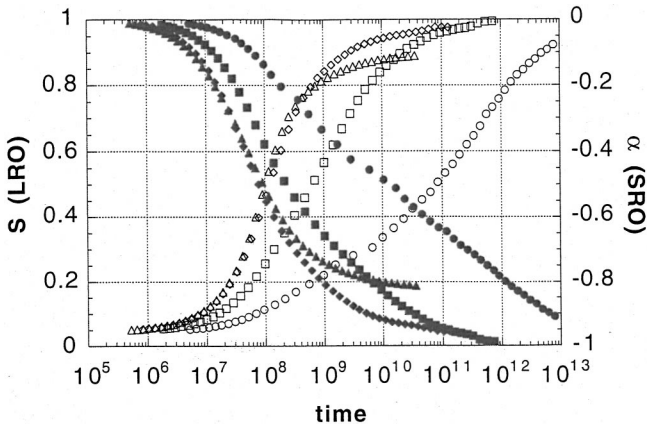

FIG. 3. Evolution of the long-range order parameter S (open symbols) and of the short-range order parameter α (solid symbols) for several temperatures: $T=0.723T_c$ (△), $T=0.542T_c$ (◇), $T=0.362T_c$ (□) and $T=0.250T_c$ (○). Time is given in arbitrary units.

below. Despite this limitation, this regime will still be referred to as the ''ordering'' regime in this paper. After this first regime, the domains coarsen [Figs. 1(c) and 2(c)] by the migration of APBs towards their center of curvature. At low temperatures [Fig. 2(c)] APBs develop facets locally, with mostly {110} and sometimes {100} orientation.

2. Apparent coarsening exponents

For a quantitative analysis, the time evolution of α, S, and L is given in Figs. 3 and 4 for four annealing temperatures: $0.723T_c$, $0.542T_c$, $0.362T_c$, and $0.250T_c$. In order to check any power-law dependence of L with time, the apparent coarsening exponent at time t, $n_{\mathrm{app}}(t)$, is calculated (Fig. 5). It is obtained from the local slope of $\log[L(t)]$ versus $\log(t)$ curves by a least-squares fit including the values of L at time t and at two iterations before and after time t. Because of the large simulation cell used here, with more than 16×10^6 atoms, very little variation in $L(t)$ is seen from one run to

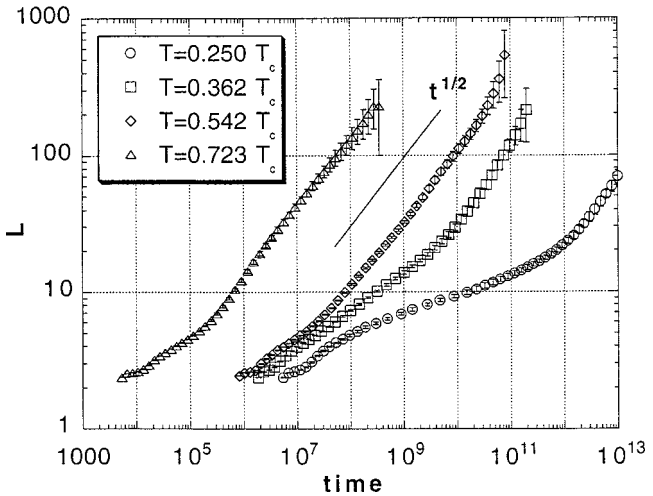

FIG. 4. Average evolution of the domain size L at several temperatures. Eight runs have been used for each temperature. The error bar corresponds to one standard deviation. L is given in bcc lattice parameter units, and time is given in arbitrary units. For clarity, the times for $T=0.723T_c$ have been divided by 100.

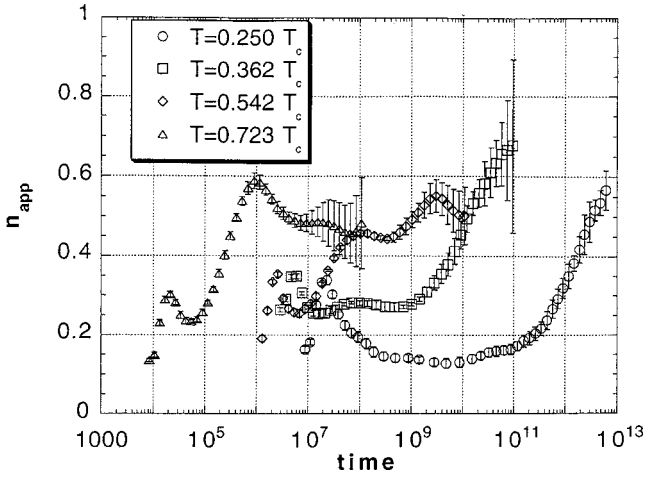

FIG. 5. Evolution of the apparent coarsening exponent $n_{app}(t)$ at several temperatures. Eight runs have been used for each temperature. The error bar corresponds to one standard deviation. Time is given in arbitrary units. For clarity, the times for $T=0.723T_c$ have been divided by 100, and for each temperature the late data are not shown when the standard deviation gets too large.

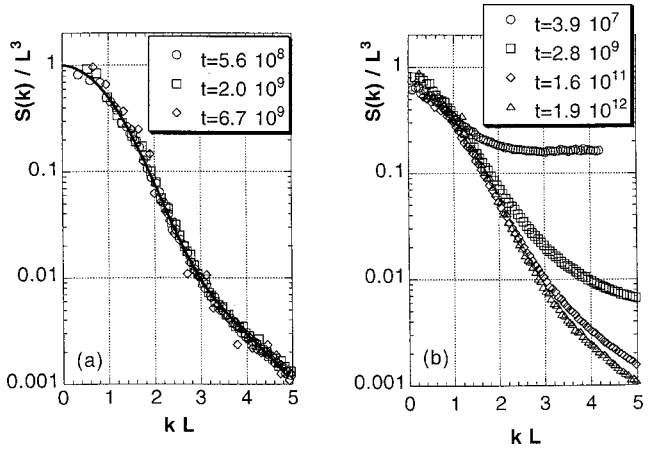

FIG. 6. Normalized scaled structure factor as a function of the scaled wave vector. (a) At $0.732T_c$ data obtained from times greater than $\sim 5.6\times 10^8$ collapse onto a single curve. The solid line corresponds to the universal scaling function proposed by Ohta *et al.* (Ref. 31). (b) At $0.254T_c$ for times $3.9\times 10^7 \leqslant t \leqslant 1.9\times 10^{12}$, dynamical scaling is not obeyed.

another until the late times, when finite-size effects and periodic boundary conditions become important, often leading to an acceleration of the coarsening. This part of the results is not representative of a bulk behavior and will not be considered here. In order to improve the statistics at intermediate times, eight runs have been cumulated for each temperature. Figures 4 and 5 display average values and variances over these eight runs.

At the highest temperature, the apparent growth exponent reaches a value of 0.59 at the end of the ordering regime ($t=10^8$); then, it stabilizes at an average value of 0.48 (for times such that $10^9<t<10^{10}$) before finite-size effects become important. A similar behavior is observed at $0.542T_c$, except that the coarsening exponent reached at the end of the ordering regime is smaller, $n_{app}=0.45$ at $t=10^8$; the average value of the coarsening exponent is 0.51 for times $10^9<t<10^{10}$. At $0.362T_c$, the end of ordering is reached at $t=2\times 10^8$, and the coarsening exponent is fairly constant over two time decades, $10^7<t<10^9$, with an average value of 0.27. Then the exponent starts to increase and a value close to 0.6 is reached when boundary conditions start to affect the results. At the lowest temperature we used, $0.250T_c$, the decrease of the coarsening exponent is even more marked. Over more than two time decades, $3\times 10^8<t<10^{11}$, the exponent is fairly constant, with an average value of 0.14. Then it increases and reaches a value around 0.55.

3. Test of dynamical scaling and anisotropy of the structure factor

In the asymptotic regime, the structure factor should obey dynamical scaling.[31] To test such scaling, the scaled structure factor $S(|\mathbf{k}-\mathbf{k}_s|,t)/L^3(t)$ is plotted as a function of the scaled module $|\mathbf{k}-\mathbf{k}_s|L(t)$. As shown in Fig. 6(a), data obtained at $0.732T_c$ for times greater than $\sim 5.6\times 10^8$ collapse onto one curve. This curve compares very well with the theoretical curve predicted by Ohta *et al.*[31] This time threshold for scaling corresponds precisely to the time when the coarsening exponent just reaches its plateau value at 0.48. At shorter times, data do not collapse onto one curve. It is not surprising that dynamical scaling does not hold during this transient. At temperature $0.542T_c$, $0.362T_c$, and $0.250T_c$ dynamical scaling is found to hold at times greater than 1.8×10^9, 1.0×10^{10}, and 7.8×10^{12}, respectively. In all cases dynamical scaling is therefore observed when the coarsening exponent has reached a value close to the Cahn-Allen 1/2 exponent. During the slow coarsening regime, dynamical scaling is not obeyed, as exemplified in Fig. 6(b) for $0.250T_c$ at times $5.2\times 10^7 \leqslant t \leqslant 2.4\times 10^{12}$.

During domain coarsening, small facets are observed at low annealing temperatures. The presence of these small facets, however, does not affect significantly the measure of $L(t)$ obtained from a spherically average structure factor. Indeed, we have also used linear averages of the structure factor along the $\langle 110\rangle^*$, $\langle 100\rangle^*$, and $\langle 111\rangle^*$ directions to calculate the domain size: the linear averages yield values for $L(t)$ that are similar to those obtained using a spherical average, as seen in Fig. 7. The slow coarsening regime is still observed with the directional averages, with a slight increase of the apparent coarsening exponent during that slow regime, e.g., from 0.25 with the spherical averages to 0.28 for the directional averages at $0.362T_c$. The statistical fluctuations on the linear averages are, however, quite large, as expected since the multiplicity of $\mathbf{k}-\mathbf{k}_s$ is reduced by a factor of the order of 256^2 by going from a spherical to a linear average for the system size we used. Simulations required to analyze in detail possible anisotropic coarsening are beyond our computing capabilities. The present results, as well as the general aspect of the microstructures, indicate, however, that if such an effect exists, it is small. More importantly, it shows that the slow coarsening regime is not an artifact due to the spherical average taken in the calculations of $L(t)$.

4. Injection and annealing of antisites

As discussed in Sec. III A 1 (see also Fig. 2), antisites in excess of their equilibrium concentration are formed at low temperatures. To quantify this evolution the number of *B*

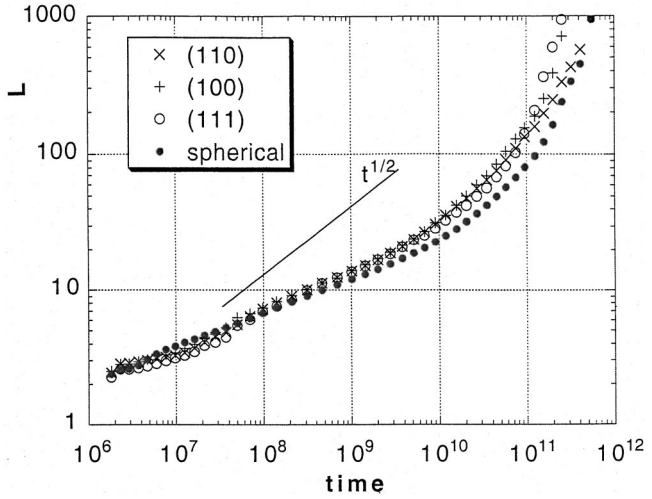

FIG. 7. Domain size as measured from structure factor after directional or spherical average for $T=0.362T_c$. Three directions have been used separately: $\langle 110\rangle^*$, $\langle 100\rangle^*$, and $\langle 111\rangle^*$ for the directional averages. Each datum represents the average of eight runs.

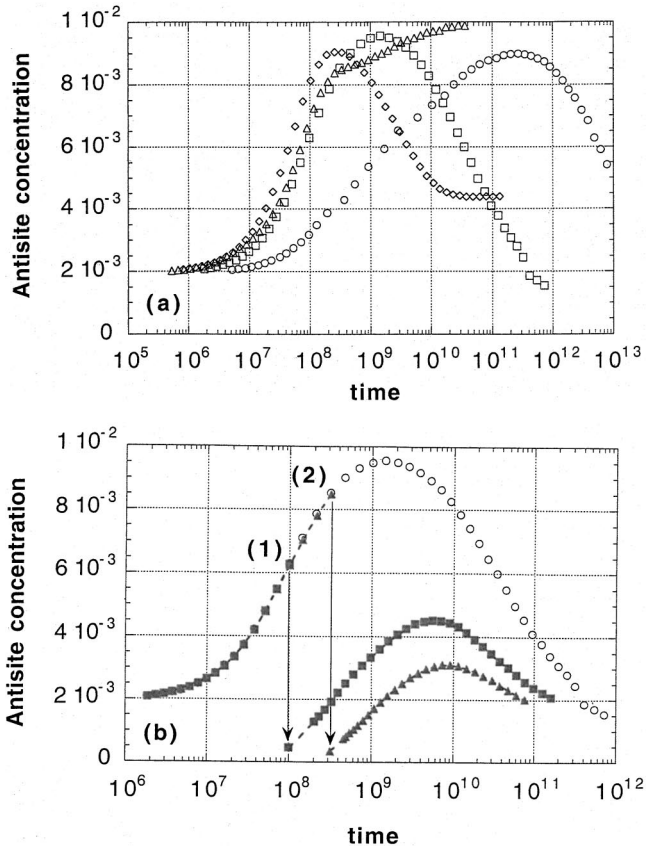

FIG. 8. Evolution of the concentration of B-atom perfect antisites (a) at various temperatures $T=0.723T_c$ (△), $T=0.542T_c$ (◇), $T=0.362T_c$ (□), and $T=0.250T_c$ (○). The equilibrium perfect antisite concentration, as measured with equilibrium Monte Carlo simulations on single-domain structure, is 9.7×10^{-3} at $T=0.723T_c$, 3.9×10^{-3} at $T=0.542T_c$, and 2.2×10^{-4} at $T=0.362T_c$. For $T=0.250T_c$ the concentration could not be measured accurately, but a low-temperature mean-field calculation yields a concentration of 2.1×10^{-5}. (b) At $T=0.362T_c$: artificial annealing of these antisites at $t=1\times10^8$, curve 1 (■), or at $t=3\times10^8$, curve 2 (▲); the reference curve (○) is also shown (arbitrary time units).

atoms having only B atoms as first nearest neighbors, hereafter referred to as B-atom perfect antisites, are measured during the simulations: as seen in Fig. 8(a), their concentration goes through a transient maximum for annealing temperatures of $0.542T_c$ and below. This transient increase becomes more pronounced and more long lived at lower temperatures. This is unexpected since the equilibrium antisite concentration decreases significantly with temperature. The maximum antisite concentration reached at $0.362T_c$ is 40 times above its equilibrium value. To better characterize this phenomenon, an annealing simulation at $0.362T_c$ is stopped during the low-$n_{\mathrm{app}}(t)$ regime (either at $t=10^8$ or $t=3\times10^8$); almost all perfect antisites are then artificially annealed out by changing the chemical nature of the antisite atoms, and the simulations are resumed: as clearly is visible in Fig. 8(b), the antisite concentration re-increases despite the artificial annealing. Direct observations of the configuration yield the explanation for this increase: it originates from the debris left over by small domains that have just annealed out and disappeared inside larger domains of the opposite variant (Fig. 9). APBs enclosing domains are locally nonconservative for most orientations. Indeed, for a boundary to locally conserve the stoichiometric composition, the (1/2,1/2,1/2) translation vector relating one variant to another has to lie in the APB plane, a condition that can also be expressed by saying that the scalar product between this vector and the vector normal to the APB is zero. For an APB enclosing a domain, this condition is only fulfilled at few places of the APB, and therefore one expects that APBs carry in general some excess of either A or B atoms. Such an excess will move with the boundary while the domain is shrinking, and it will remain as antisite debris after the disappearance of the domain. Because of composition imbalance in these debris, some long-range diffusion is required to anneal them. At early stages of coarsening, many domains disappear per unit time, resulting in a transient increase of antisites. This increase is more pronounced at low temperatures because atomic mobility becomes slower and it takes more time for the vacancy to transport these antisites inside ordered domains and let them recombine. An important correlation has to be noticed here: as seen from Figs. 5 and 8(a), the time intervals during which a low coarsening exponent is measured coincide with those during which the antisite concentration increases, e.g., $10^7<t<10^9$ at $0.362T_c$. Furthermore, when no transient excess antisite is measured, e.g., at $0.723T_c$, the coarsening exponent is very close to 1/2. Visualization of configurations at low temperatures after the artificial antisite annealing reveals another effect: antisites in excess left by disappearing domains are removed at later times by the sweeping of other APBs moving through these areas (Fig. 9). This appears to become the predominant mechanism for the elimination of excess antisites at low temperatures. This is not surprising since, with the current simulation parameters, vacancies segregate at APBs at low temperatures and since migration barriers are reduced at APBs, by as much as a factor of 2. At these low temperatures the evolution of antisites therefore results from a competition between their creation by domain disappearance and their

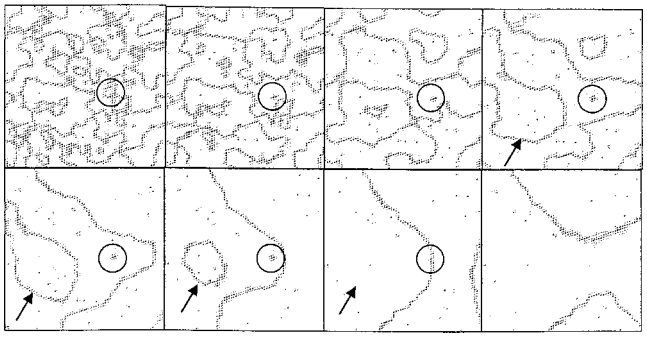

FIG. 9. Snapshots of the absolute value of the local degree of the order field at $T=0.362T_c$, after an artificial annealing of antisties at $t=3\times10^8$ [curve 2 in Fig. 8(b)]. Time increases from left to right and from top to bottom, the initial and final times being 6.1×10^8 and 6.0×10^{10} (arbitrary units). Notice at earlier times the formation of chemical disorder inside domains by the disappearance of smaller domains (e.g., see the circled region) and at later times the partial annealing of this disorder when APBs sweep through these areas (e.g., see the circled region or the domain indicated by the arrow). The vertical dimension of each microstructure corresponds to 64 nearest-neighbor distances, the simulation cell still containing 256^3 sites.

annihilation by APB sweeping. This may explain why the domain size at which the antisite concentration is maximum is $L\approx15$ for both $0.362T_c$ and $0.250T_c$ despite the large difference in the annealing times, $t=1.5\times10^9$ and $t=2.5\times10^{11}$, respectively.

The main results of Sec. III A can be summarized as follows. In the late stages of coarsening, as expected from the Allen-Cahn theory, a power-law regime for $L(t)$ with an exponent very close to 0.5 is found in our simulations for temperatures above $0.5T_c$ and the structure factor obeys isotropic dynamical scaling. Below $0.5T_c$ temperature, the final value of the slope is compatible with the theoretical value, but no well-defined plateau has been reached for the coarsening exponent. Larger system sizes and longer simulation times would be necessary to really assess this long-time behavior. The ''ordering'' stage and the beginning of the coarsening stage are, however, strongly slowed down at these low annealing temperatures. In these time intervals $S(\mathbf{k})$ does not obey dynamical scaling and the concentration of antisites increases well above its equilibrium value. This increase is due to the combination of two factors: the disappearance of antiphased domains and the slow bulk atomic mobility at low temperatures. Let us stress that the slow coarsening does not reduce itself to a decrease of the APB mobility at low temperature: this would shift the $L(t)$ curves to longer times, but should not affect the apparent coarsening exponent. In fact, at the lowest temperature, $0.250T_c$, the average exponent is so small that the $L(t)$ curve could almost be approximated by a logarithmic dependence. This long-lived slowing down, associated with a low apparent coarsening exponent, is not predicted by any existing theory. It constitutes the main result of this paper. Our objective in the following sections is to elucidate the origin of this anomalous slow kinetics.

B. Effect of alloy composition

In this section we investigate the effect of the alloy composition on the slowing down that has been identified at low

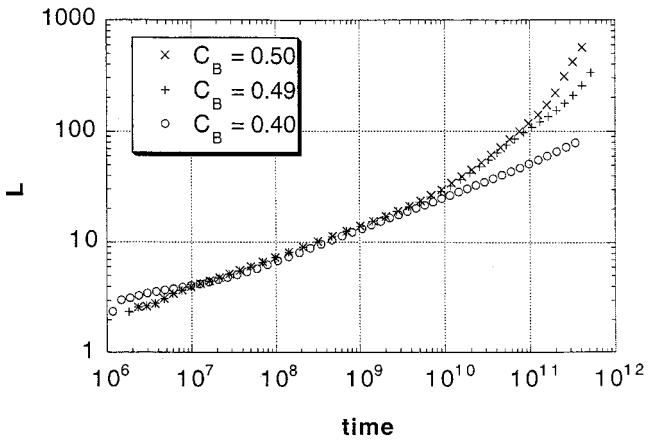

FIG. 10. Evolution of the domain size L at $T=0.362T_c$ for several compositions. L is given in bcc lattice parameter units, and time is given in arbitrary units.

annealing temperatures in the previous section. Two nonstoichiometric compositions have been studied, with 40% and 49% of B atoms, and compared to the stoichiometric composition. Figures 10 and 11 display the evolutions of $L(t)$ and $n_{\mathrm{app}}(t)$ for the three alloys for an annealing temperature of $0.362T_c$. Remarkably enough, in the regime where the slowing down is observed for the stoichiometric alloy, the evolution of the three alloys is almost identical. It is also concluded by visualization of the configurations and by inspection of the small-$\mathbf{k}$ behavior of the structure factor that no noticeable segregation has yet developed for any of the alloys in this regime. This similarity in the evolution of the three alloys is consistent with the Monte Carlo results obtained by Porta and Castán[32] on a binary alloy with no vacancy. At the end of the slowing down, $t\approx10^9$, the near-stoichiometric alloy still follows the evolution of the stoichiometric one, until finite-size effects become important ($t>10^{11}$). The 40% alloy, however, exhibits only a modest increase of the exponent $n_{\mathrm{app}}(t)$, which takes an average value of 0.32 when $t>10^{10}$. In this regime, significant segregation is observed at APBs. Similar results are observed at $0.250T_c$.

It could be tempting to interpret the results obtained for nonstoichiometric alloys in the light of the models proposed

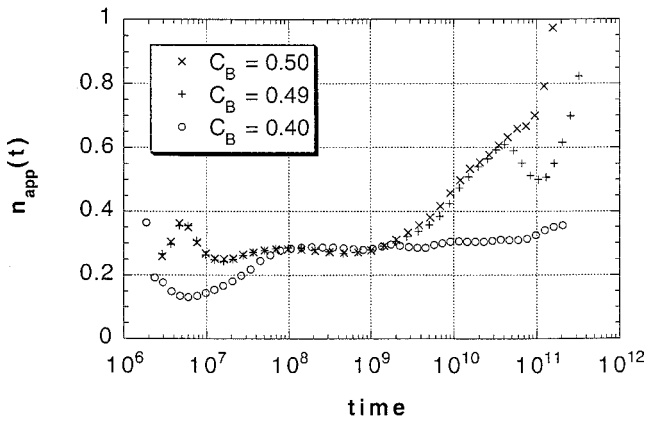

FIG. 11. Evolution of the apparent coarsening exponent $n_{\mathrm{app}}(t)$, at $T=0.362T_c$ for several compositions. Time is given in arbitrary units.

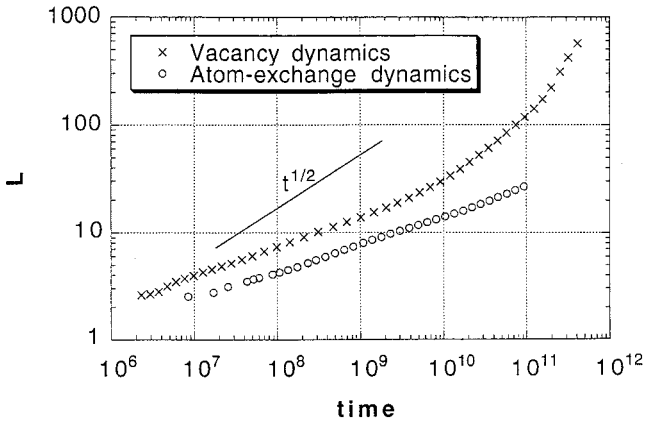

FIG. 12. Evolution of the domain size L, at $T=0.362T_c$ for the vacancy dynamics ($\times$) and for the direct atom-exchange dynamics ($\bigcirc$). L is given inpop bcc lattice parameter units. Different arbitrary time units are used in the two curves.

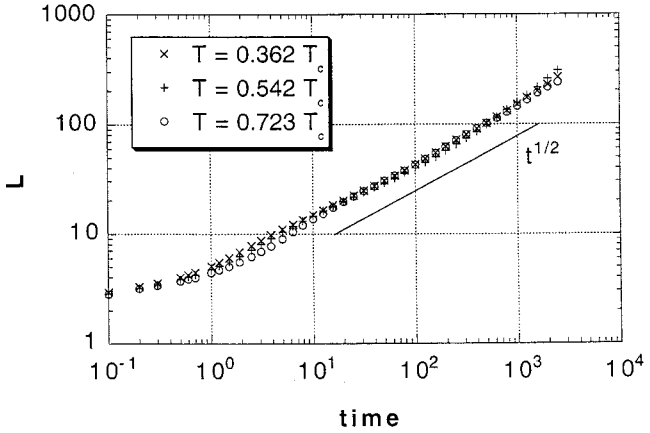

FIG. 13. Evolution of the domain size L with a spin-flip dynamics at several temperatures. Notice that for this dynamics, temperature does not alter the coarsening regime ($10^1<\text{time}<10^3$). Time is given in Monte Carlo steps, i.e., in the number of spin-flip attempts per site. In these simulations, no vacancy is present in the crystal.

by Krzanowski and Allen[7] or Dobretsov *et al.*[8] In both cases, however, equilibrium segregation is required to affect the APB mobility and no effect is predicted for stoichiometric alloys. Therefore we conclude that these approaches are not appropriate to rationalize our results at early stages for both stoichiometric and nonstoichiometric alloys.

Finally, let us stress that wetting does not occur in our simulations since for all compositions and temperatures studied here alloys at equilibrium are single-phase $B2$. The fact that the late stage coarsening exponent for the 40% alloy is very close to 1/3 is, in our opinion, fortuitous. This low coarsening exponent could well correspond to the effects predicted by Dobretsov *et al.*[8] for nonstoichiometric alloys since it takes place when segregation has built up at APBs. A detailed study of the late-time coarsening in nonstoichiometric alloys is, however, beyond the scope of this paper.

C. Effect of atom dynamics

In order to gain more insight into the origin of the slowing down observed at low temperatures, different modifications are now made to the atomic kinetic model presented in Sec. II. The atomic dynamics considered so far has two important characteristics: (i) it conserves the composition of the alloy at each Monte Carlo step and (ii) it can be affected by vacancy segregation (or trapping) at different regions of the microstructure (e.g., inside a perfectly ordered domain, next to an antisite atom, or at an APB). In order to assess the impact of these characteristics on the anomalous slow kinetics at low temperatures, other dynamics have been implemented: First, a direct atom-exchange dynamics, then a ''spin-flip'' dynamics. In both cases, vacancies are no longer used, and therefore the kinetics is free from possible vacancy trapping effects. Furthermore, in the ''spin-flip'' dynamics case, the composition is no longer locally conserved and thus composition fluctuations can be annealed out without requiring long-range atom transport.

The direct atom-exchange mechanism (also known as a Kawasaki dynamics[33]) has been implemented following the algorithm described by Salomons *et al.*[34] Figure 12 compares the $L(t)$ curves obtained at $0.362T_c$ with the vacancy dynamics and with the direct atom-exchange dynamics: both dynamics result in a ''slow'' ordering and coarsening, with almost identical exponents in the power-law fits. Similar results have already been obtained by Athènes[22] over a broad temperature range. Notice that the two time scales do not have to be identical because of the specifics of jump and exchange frequencies used in the models. Direct visualization of the configurations and antisite concentration measurements reveals that, similarly to the vacancy dynamics case, a large excess of antisite develops inside the ordered domains, giving rise to a transient increase of the antisite concentration.

Then the ordering of the alloy is modeled by using the classical ''spin-flip'' mechanism, i.e., by replacing A or B atoms by B or A atoms, according to a Metropolis acceptation probability.[35] This dynamics, which has been widely used to model magnetic phase transformations, is clearly not appropriate for describing diffusion-controlled transformations, since it does not conserve locally the composition of the alloy. The results are, however, very instructive. Figure 13 displays the evolution of $L(t)$ at $0.723T_c$, $0.542T_c$, and $0.362T_c$: it is quite clear that there is little, if any, temperature effect with the spin-flip dynamics. Furthermore, at times greater than ten Monte Carlo steps and before the acceleration due to finite-size effects, the average coarsening exponents are 0.52, 0.51, and 0.50, for high, intermediate, and low temperature, respectively. Direct visualization of the configurations and antisite concentration measurements shows that, for this atom dynamics, the degree of order inside the domains quickly reaches a value very close to the equilibrium one and that no transient maximum develops for the antisite concentration, even at low temperatures. This is another noticeable difference with the microstructures obtained with the vacancy and with the direct atom-exchange mechanisms.

IV. DISCUSSION

At high annealing temperatures, domain coarsening in our simulations closely follows the Allen-Cahn law. At lower temperatures ($T\leqslant 0.5T_c$), the long-time behavior seems also

to be in agreement with the Allen-Cahn coarsening exponent, but larger system sizes and longer simulation times would be required to firmly establish such a result. The main surprising result is that systems at low temperatures exhibit a transient slow coarsening regime that follows an apparent power-law behavior. The apparent exponent of this transient decreases with decreasing annealing temperature. The possible origins of this slowing down, as well as its implications, are now discussed. Since the slowing down starts more or less at the beginning of the coarsening stage and since coarsening theory is far more developed than that of ordering, we will discuss this anomalous behavior in the light of existing coarsening theories.

For that purpose, let us first stress that the Allen-Cahn law rests on several assumptions: (i) the principal radii of curvature of APB are large compared to their thickness, (ii) the degree of order has reached its bulk equilibrium value inside the domains and its local equilibrium value near or at an APB, and (iii) the domain microstructure is invariant by scaling during the growth process. At low temperatures where a slowing down is observed in the simulations, the above three assumptions are in fact violated: As seen in Fig. 2(b), for instance, there are many places where the local radius of curvature is comparable to the width of an APB; the degree of order inside the domains has not reached its equilibrium value, as discussed in Sec. III A; finally, the APBs develop facets, predominantly with {110} and {100} orientations, leading to microstructures which are most likely no longer scale invariant; the faceting of APB is not surprising since the annealing temperatures are below the equilibrium roughening temperatures, which have been determined to be $0.44T_c$ and $0.76T_c$ for {110} and {100} orientations, respectively.[36] We will now determine which of the above three points [(i), (ii), or (iii)] contributes to the slowing down. One can safely eliminate the first point as a dominant factor: this point is also not satisfied during the early stages of coarsening with the ''spin-flip'' dynamics, without resulting in any significant slowing down. In fact, we show now that point (ii) is sufficient to explain in a consistent way all the simulation results we have presented so far.

As discussed in Sec. III A, the coarsening of ordered domains can both decrease or increase locally the degree of order: the disappearance of a domain results in additional antisites, whereas a moving APB removes excess antisites along its wake. At low temperatures atomic mobility is low because of the trapping that vacancies are experiencing in highly ordered regions.[21] As a result, the above contributions of APBs to the evolution of the degree of order field become predominant. At the beginning of the coarsening, many ordered domains disappear per unit time, while the total area swept by their APBs is small: this leads to an increase of antisite concentration, as observed in the simulations [see Fig. 8(a)]. At short time scales this excess of antisites is expected to lower the mobility of APBs, either by analogy with the solute-drag effect or by considering these excess antisites as quenched impurities.[37] Such a suppression of APB mobility has also been observed in the presence of equilibrium segregation.[8] At later times the antisite excess should disappear by the recombination of antisites at APBs. Accordingly, in the time interval during which the antisite concentration increases, e.g., $10^7 < t < 10^9$ at $0.362T_c$, the

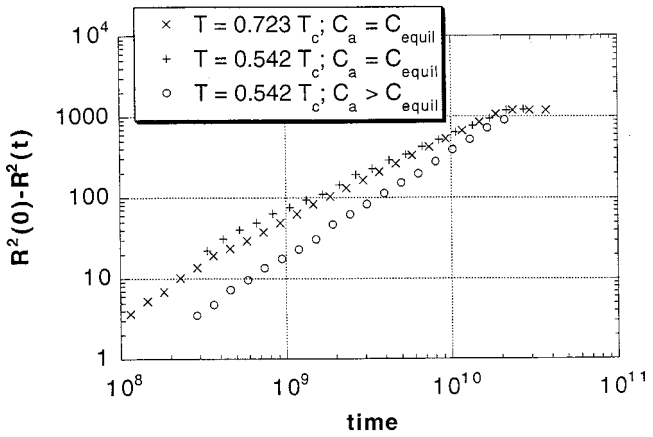

FIG. 14. Relative decrease of the squared radius of a spherical antiphase domain $R^2(t)$ at several temperatures. When the initial concentration of *B*-atom perfect antisites is set close to its equilibrium value, $C_a = 4.4 \times 10^{-3}$ at $T = 0.542T_c$ (+) and $C_a = 1.0 \times 10^{-2}$ at $T = 0.723T_c$ (×), the decay is nearly linear in time. At $T = 0.542T_c$, with an initial antisite concentration of $C_a = 1.9 \times 10^{-2}$ (○) the decay is no longer linear and is initially slowed down. R is given in bcc lattice parameter units.

APB mobility should continuously decrease, and therefore the coarsening kinetics should slow down. As already stressed in Sec. III A, such a one-to-one correlation between antisite increase and slow coarsening is indeed observed in the simulations; it provides a strong indirect argument in favor of the mechanism we just proposed.

A key component of our rationalization of the slow coarsening regime is the assumption that the APB mobility decreases with increasing antisite concentration. We will now establish this coupling by performing additional simulations where we follow the decay of a large spherical antiphase domain in a single-domain matrix. Antisites are initially introduced homogeneously, with a concentration set to a chosen value, either the equilibrium concentration for the temperature studied or a nonequilibrium concentration. The decay of the radius of this spherical domain, as well as the *B*-atom antisite concentration $C_a(t)$, are then measured by using kinetic Monte Carlo simulations with the vacancy-jump dynamics. According to the Allen-Cahn law, the square of the radius of the domain, R^2, should decrease linearly in time, the coefficient being proportional to the APB mobility. The linear decay of R^2 is indeed observed in Fig. 14 for annealing temperatures of $0.723T_c$ and $0.542T_c$ when the antisite concentration is initially set to its equilibrium value. However, an initial excess of the concentration of antisites over its equilibrium value leads to an initially slower decay of the spherical antiphase domain, as shown in Fig. 14 at a temperature of $0.542T_c$. During such simulations, atomic diffusion is still efficient enough to remove, however slowly, this excess of antisites. We have checked that this annealing process takes place homogeneously and that the domain remains spherical during its decay. In these simulations the antisite concentration decreases with time, whereas during the annealing of quenched configurations (Sec. III), a transient increase of antisites is observed. Since time in itself is irrelevant to the transient mobility of the spherical APB, it is useful to eliminate the time variable between the $dR^2(t)/dt$ and $C_a(t)$ evolutions, so as to extract an effective APB mo-

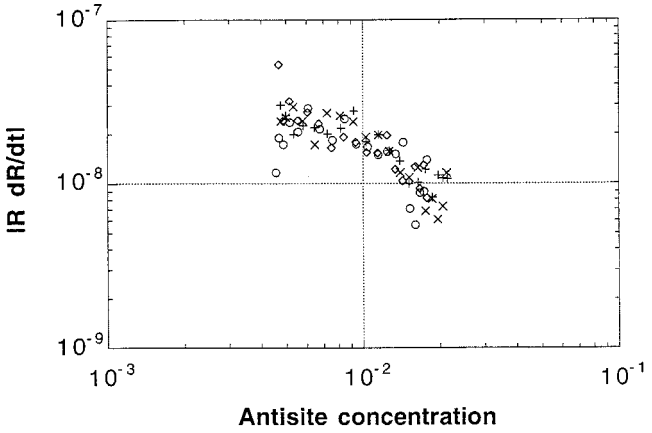

FIG. 15. Evolution of $|R\,dR/dt|$ at $T=0.542T_c$ as a function of the B-atom perfect antisite concentration. As in Fig. 14, $R(t)$ is the radius of a decaying spherical antiphase domain. $|R\,dR/dt|$ yields an apparent APB mobility. Four runs are represented obtained with different initial antisite concentrations. Despite the dispersion in the results, the apparent APB mobility is clearly reduced by an excess of antisites (the equilibrium value is $C_a=3.9\times10^{-3}$ at this temperature).

bility as a function of the antisite concentration. As seen in Fig. 15, this procedure reveals clearly the effect of excess antisites on APB mobility, the latter being roughly inversely proportional to the antisite concentration. At lower temperatures a decrease of the APB mobility with increasing antisite concentration is also clearly observed. However, vacancy trapping results in quite large fluctuations from run to run, and even after averaging over 20 runs, we were not able to determine quantitatively this APB mobility dependence. Such a quantitative information would be required if one were to model the decrease of the apparent coarsening exponent as a function of the annealing temperature. This is beyond the scope of this paper.

We now briefly establish that point (iii), the faceting of APBs, cannot alone explain the slowing down we are reporting here. As discussed in the Introduction, the presence of facets may result in a slower kinetics. However, we have found apparent coarsening exponents that take values below 1/4. This indicates that the analysis proposed by Castan and Lindgard[2] probably does not apply here. Furthermore, activation barriers to nucleate and propagate a kink along a facet edge can be calculated for the vacancy-assisted diffusion model and for the ''spin-flip'' dynamics used in Sec. III C: for both models the barrier is independent of the length of the facet (because of the absence of second-nearest-neighbor interactions). According to the classification by Lai, Mazenko, and Valls,[3] our model is thus a class-2 model, and domain coarsening should follow the classical Allen-Cahn behavior. Finally, if faceting were to play an important role in coarsening, anisotropic coarsening should be observed both in direct and reciprocal space, as, for instance, in the work by Porta *et al.*[18] Directionally averaged structure factors (see Sec. III A 3) are instead consistent with a mostly isotropic coarsening regime. We thus conclude that faceting alone cannot explain the slow coarsening observed at low temperatures; it may, nevertheless, play some role in the dependency of APB mobility with antisite concentrations.

Let us now show that all simulation results reported here are well rationalized with the explanation we just proposed for the slow coarsening regime. This explanation is based on the conjunction of three factors: the injection of antisites due to domain disappearance, the slow diffusivity of antisites inside ordered domains, and an APB mobility that decreases with increasing antisite concentration. Accordingly, the slow regime for coarsening should present the following characteristics: It should be only transient since the antisite concentration inside ordered domains will eventually reach its equilibrium value, it should be more pronounced at lower temperatures, and it should be observed only with atom dynamics that conserve locally the composition, but should not be specific to a vacancy mechanism. It should also be observed in nonstoichiometric alloys before any segregation has developed, since one family of antisites will develop an excess, which would result in a lower APB mobility. All these characteristics are indeed observed in our simulations, except for the firm proof that the true asymptotic regime at low temperatures is the classical Allen-Cahn one. The mechanism we have proposed to account for the observed transient slow coarsening is by no means specific to the $B2$-ordered structure investigated in this paper. Similar transients should take place in other ordered structures, provided that the three conditions listed above are met. The temperatures at which such transients would appear and their apparent coarsening exponents would, however, clearly vary from one alloy to another. The mechanism proposed here provides a simple rationalization for the low coarsening exponents obtained by Frontera *et al.*[17] for an $L1_2$ ordering at $0.55T_c$, with a direct-exchange mechanism and a vacancy mechanism (see Sec. I).

No systematic experimental study of the effect of annealing temperature on coarsening has been performed, because of the long annealing times it would require for most known alloys. A direct check of the slow coarsening regime reported here is therefore not currently possible. It is, however, worth noting that in the recent detailed study of ordering and coarsening kinetics in Fe_3Al by Park *et al.*,[12] at temperatures below $0.95T_c$ the correlation length of short-range order (SRO) fluctuations initially increases and goes through a transient maximum before reaching its equilibrium value. This phenomenon is particularly clear at the lowest temperature studied, 757 K, i.e., $0.92T_c$, where the SRO correlation length reaches a maximum value around 20 Å, even though its equilibrium value at this temperature is near 2 Å. In the light of our simulations, these observations could well correspond to a transient increase in antisites, as reported in Sec. III A. The transient increase in the simulations is clearly detected only at temperatures below $0.6T_c$, but this threshold temperature should vary from one alloy to another since it depends significantly on the ordered phase involved and on the mobility of antisite atoms. This transient behavior is not easily accessible experimentally because it is not associated with a transient extremum of the SRO parameter (see Fig. 3). The absolute value of the SRO increases continuously for all annealing temperatures, since ordering and the disappearance of APBs are the predominant factors in the measure of the SRO.

From a practical point of view, the transient slow coarsening regime reported here has important consequences: at low annealing temperatures this transient regime may be the

only one accessible experimentally, and therefore one should not always expect the average domain size to coarsen as $t^{1/2}$. It also implies that one cannot safely extrapolate coarsening rates obtained at high temperature to low temperatures. As seen in Fig. 4, the time required to reach a given domain size can be delayed by several orders of magnitude. In order to test these points and the simulation results presented here, there is a clear need for new coarsening experiments performed at low temperatures.

V. CONCLUSION

Kinetic Monte Carlo simulations relying on an vacancy-atom-exchange kinetic model and a residence time algorithm have been performed to study the ordering and coarsening of $B2$ domains during isothermal annealing of a quenched disordered phase. For annealing temperatures above $\approx 0.5T_c$, a coarsening exponent very close to the classical Allen-Cahn value of 1/2 is measured. For lower temperatures, however, a transient coarsening regime is observed with an apparent coarsening exponent that decreases with decreasing temperature. It is associated with in a severe slowing down of the domain coarsening kinetics. This effect is shown to be present for both stoichiometric and nonstoichiometric alloys. Atom dynamics not relying on vacancy-atom exchange are also used for comparison: a slow transient is also observed for a direct atom-exchange dynamics, but not for a spin-flip dynamics. Based on the results presented in this paper, the following mechanism is proposed to account for this slow transient coarsening regime. Domain annealing and disappearance lead to the injection of antisite atoms, which are difficult to eliminate at low temperatures. This results in a transient increase of the excess of antisite defects inside ordered domains. Since the mobility of APBs is shown to be reduced by an excess of antisites, the coarsening is slowed down, until this excess of antisites is annealed out, either by atomic diffusion or by an ''APB sweeping'' effect observed in the simulations. The generality of these arguments predicts that similar slow transient coarsening regimes should be observed in other ordered structures.

ACKNOWLEDGMENTS

This work has been supported by the U.S. Department of Energy, Basic Energy Sciences, Grant No. DEFG02-967ER45439 through the University of Illinois Materials Research Laboratory. The present simulation work has greatly benefited from the MRL Center for Computation.

*Present address: DSM/SRSIM, CEA-Saclay, Gif-sur-Yvette, 91191, France.
†Corresponding author. FAX: (217) 333-2736.
Email: bellon@uiuc.edu

[1] S. M. Allen and J. W. Cahn, Acta Metall. **27**, 1085 (1979).
[2] T. Castan and P.-A. Lindgard, Phys. Rev. B **40**, 5069 (1989); **41**, 4659 (1990).
[3] Z. W. Lai, G. F. Mazenko, and O. T. Valls, Phys. Rev. B **37**, 9481 (1988).
[4] J. D. Shore, M. Holzer, and J. P. Sethna, Phys. Rev. B **46**, 11 376 (1992).
[5] B. Fultz, Philos. Mag. A **70**, 607 (1994).
[6] M. Papoular, D. Camel, and F. Bley, Philos. Mag. Lett. **69**, 247 (1994).
[7] J. E. Krzanowski and S. M. Allen, Acta Metall. **34**, 1035 (1986); **34**, 1045 (1986).
[8] V. Yu Dobretsov, G. Martin, F. Soisson, and V. G. Vaks, Europhys. Lett. **31**, 417 (1995).
[9] J. E. Krzanowski and S. M. Allen, Acta Metall. **31**, 213 (1983).
[10] C. Frontera, E. Vives, and A. Planes, Z. Phys. B: Condens. Matter **96**, 79 (1994).
[11] S. E. Nagler, R. F. Shannon, Jr., C. R. Harkless, M. A. Singh, and R. M. Nicklow, Phys. Rev. Lett. **61**, 718 (1988).
[12] B. Park, G. B. Stephenson, S. M. Allen, and K. F. Ludwig, Jr., Phys. Rev. Lett. **68**, 1742 (1992).
[13] V. K. Vasudevan, H. P. Kao, C. R. Brooks, and E. E. Stansbury, Metall. Trans. A **19**, 941 (1988).
[14] G. E. Poquette and D. E. Mikkola, Trans. Metall. Soc. AIME **245**, 743 (1969).
[15] M. K. Phani, J. L. Lebowitz, M. H. Kalos, and O. Penrose, Phys. Rev. Lett. **45**, 366 (1980).
[16] E. Vives and A. Planes, Phys. Rev. Lett. **68**, 812 (1992); C. Frontera, E. Vives, and A. Planes, Phys. Rev. B **48**, 9321 (1993).
[17] C. Frontera, E. Vives, T. Castan, and A. Planes, Phys. Rev. B **55**, 212 (1997).
[18] M. Porta, C. Frontera, E. Vives, and T. Castan, Phys. Rev. B **56**, 5261 (1997).
[19] M. Porta, E. Vives, and T. Castan, Phys. Rev. B **60**, 3920 (1999).
[20] T. A. Abinandanan, F. Haider, and G. Martin, Acta Mater. **46**, 4243 (1998).
[21] M. Athènes, P. Bellon, and G. Martin, Philos. Mag. A **76**, 565 (1997).
[22] M. Athènes, Ph.D. thesis, University of Paris VI, 1997.
[23] D. Lefloc'h, M. Athenes, and P. Bellon, in *Phase Transformations and Systems Driven Far From Equilibrium*, edited by E. Ma *et al.*, MRS Symposia Proceedings No. 481 (Materials Research Society, Pittsburgh, 1998), p. 219.
[24] M. Athènes, P. Bellon, G. Martin, and F. Haider, Acta Mater. **44**, 4739 (1996).
[25] H. Ackermann, G. Inden, and R. Kikuchi, Acta Metall. **37**, 1 (1989).
[26] F. Soisson, A. Barbu, and G. Martin, Acta Mater. **44**, 3789 (1996).
[27] C. Pareige, F. Soisson, G. Martin, and D. Blavette, Acta Mater. **47**, 1889 (1999).
[28] S. M. Allen and J. W. Cahn, Acta Metall. **24**, 425 (1976).
[29] A. G. Khachaturyan, T. F. Lindsey, and J. W. Morris, Jr., Metall. Trans. A **19**, 249 (1988).
[30] B. Chakraborty and Z. Xi, Phys. Rev. B **53**, 5063 (1996).
[31] T. Ohta, D. Jasnow, and K. Kawasaki, Phys. Rev. Lett. **49**, 1223 (1982).
[32] M. Porta and T. Castán, Phys. Rev. B **54**, 166 (1996).
[33] K. Kawasaki, in *Phase Transitions and Critical Phenomena*, edited by C. Domb and M. S. Green (Academic, London, 1972), Vol. 2, p. 443.
[34] E. Salomons, P. Bellon, F. Soisson, and G. Martin, Phys. Rev. B **45**, 4582 (1992).
[35] N. Metropolis, A. W. Rosenbluth, M. N. Rosenbluth, A. H. Teller, and E. Teller, J. Chem. Phys. **21**, 1087 (1953).
[36] D. Le Floc'h *et al.* (unpublished).
[37] P. J. Shah and O. G. Mouritsen, Phys. Rev. B **41**, 7003 (1990).